Journal of Alloys and Compounds 521 (2012) 121–125

Contents lists available at SciVerse ScienceDirect

Journal of Alloys and Compounds

journal homepage: www.elsevier.com/locate/jallcom

CdI_2 structure type as potential thermoelectric materials: Synthesis and high temperature thermoelectric properties of the solid solution TiS_xSe_{2-x}

Franck Gascoin*, Nunna Raghavendra, Emmanuel Guilmeau, Yohann Bréard

Laboratoire CRISMAT UMR 6508 CNRS ENSICAEN, 6 boulevard du Maréchal Juin, 14050 Caen Cedex 04, France

ARTICLE INFO

Article history:
Received 6 December 2011
Received in revised form 6 January 2012
Accepted 12 January 2012
Available online 28 January 2012

Keywords:
Thermoelectric
CdI_2 type structure
Titanium selenide
Titanium sulfide
Solid solution

ABSTRACT

Polycrystalline samples of the solid solution TiS_xSe_{2-x} with x varying from 0 to 2 were prepared using direct high temperature reaction of stoichiometric amounts of the elements. Rietveld refinements of powder X-ray diffraction data are consistent with the existence of a full solid solution. High temperature Seebeck coefficient, electrical resistivity and thermal diffusivity measurements were performed on pellets densified by spark plasma sintering. These measurements reveal that along the solid solution the transport properties vary from the rather metallic and p-type character of $TiSe_2$ to the semiconducting and n-type of TiS_2. This change of conduction regime is responsible for the peculiar evolutions of transport properties of $TiS_{0.5}Se_{1.5}$ with increasing temperature that vary somewhat differently than that of the other members of the solid solution. As expected, the disorder generated by the mixed occupancy of the S and Se on the anionic site is responsible for the diminution of the lattice thermal conductivity. A maximum zT above 0.4 at 400 °C is reached for $TiS_{1.5}Se_{0.5}$.

1. Introduction

Thermoelectricity is nowadays considered as a plausible way to produce "clean" electrical energy from virtually any kind of waste heat [1]. However, the need for always higher device efficiency combined with the mandatory lowering of the cost of the watt thermoelectrically produced, help maintaining upstream material research. Material development thus passes by the discovery of novel phases. In fact, the past few years have witnessed the emergence of new families of compounds, some of which are now regarded as promising thermoelectric materials. It is the case of certain Zintl phases such as $Yb_{14}MnSb_{11}$ and its derivative for high temperature spatial applications [2–6], or some members of the $CaAl_2Si_2$ structure type [7–12]. Other such new families are the molybdenum selenides based on Mo_9Se_{11} clusters [13], and layered sulfides [14,15], oxyselenides [16] or selenides [17]. The other route to reach efficient materials, also the object of many efforts worldwide, is by optimizing the properties of known good thermoelectric materials such as Bi_2Te_3, PbTe, or SiGe for example. Today, the most "*à la mode*" utilized method is probably by way of nano-engineering aiming at decreasing the lattice contribution to the thermal conductivity κ to further increase the thermoelectric figure of merit zT defined as $\alpha^2T/\rho\kappa$ with α the Seebeck coefficient, ρ the electrical resistivity, and T the absolute temperature. To reach such an objective there are two general routes, the synthesis of nano-powders followed by their fast densification usually by spark plasma sintering to form nano-structured materials, or the introduction of nano-domains within a classical, *e.g.*; not nanometric, bulk thermoelectric matrix. The production of these nano-objects or nano-domains can be achieved by different methods including melt-spinning [18], ball-milling [19], microwave processing [20], solid state precipitation [21], spinodal decomposition [22], or solution chemistry [23]. More recently, another way has been demonstrated to improve the material performances, using band structure engineering like by introducing thallium in PbTe thus distorting the electronic density of state [24], or in Na-doped $PbTe_{1-x}Se_x$ taking advantage of the convergence of electronic bands [25].

No matter what method is used in the quest for efficient thermoelectric materials, one common prerequisite for the material is its propensity to incorporate impurities. In other words, if the thermoelectric properties can be optimized it is often through substitution or doping, meaning that the crystal structure of the considered phase must be flexible enough to be capable of accommodating all sorts of impurity such as dopants, nano-particles, nano-domains or simply to easily form solid solutions. For these reasons, it appears that layered structures are ideal candidates that could fulfill all these conditions. For example, several compounds crystallizing in the layered structures type $CaAl_2Si_2$ and CdI_2 have respectable thermoelectric properties and more importantly demonstrate that there is a great deal of compounds susceptible of possessing interesting thermoelectric properties precisely because of the flexibility

* Corresponding author. Tel.: +33 231 452 605; fax: +33 231 951 600.
E-mail address: franck.gascoin@ensicaen.fr (F. Gascoin).

0925-8388/$ – see front matter © 2012 Elsevier B.V. All rights reserved.
doi:10.1016/j.jallcom.2012.01.067

of the structures and thus because of the numerous chemical compositions that can adopt such adaptable structures [7–12,15,17]. In these structures, whereas various species can be intercalated between the layers, it is also often possible to introduce compositional disorder within the layer itself by using multiple cations (transition metals) and/or multiple anions. We have thus embarked in the systematic studies of transition metal heavy chalcogenides. Herein, we report on the synthesis and thermoelectric properties of the intercalate-free solid solution TiS_xSe_{2-x} with $x = 0$, 0.5, 1, 1.5, and 2, family of phases that indeed illustrate the multitude of combinations offered by such a structure to tune the transport properties.

2. Experimental

2.1. Synthesis

The title compounds were prepared directly from stoichiometric mixture of the pure elements. Typically, 7 g batches were prepared from titanium powder (−325 mesh, 99%, Alfa Aesar), sulfur powder (−325 mesh, 99.5%, Alfa Aesar) and selenium shots (99.999% Alfa Aesar) used as received. The mixes were loaded in fused silica ampoules flame sealed under vacuum. These assemblies were then placed vertically in box furnaces. The temperature was raised from room temperature to 500 °C at 50 °C/h, kept at 500 °C for 2 h and then raised (with the same rate) to 650 °C, temperature at which the ampoules stayed for 12 h. Finally, the furnaces were allowed to cool to room temperature in 12 h. After this thermal cycle, all the products look like homogeneous fine green to gray powders.

2.2. Densification

In order to obtain dense samples, finely ground powders of each of the title compounds were sieved down to 200 μm. About 6 g of each sample were then inserted in high density graphite dies (Carbonloraine) with an inner diameter of 15 mm. The densification was performed using a spark plasma sintering (FCT HP D 25/1). The temperature was raised at 100 °C/min to 800 °C, it was then kept at that temperature for 30 min before the samples were cooled down to room temperature over a period of 30 min. A pressure of 50 MPa, applied before raising the temperature, was kept constant during the 800 °C plateau and was allowed to decrease over the cooling period. The densities of the resulting pucks, determined by the Archimedes method using ethanol as the displaced fluid, were higher than 95% of the theoretical densities.

2.3. Characterization

The structural characterization has been carried out by means of a Panalytical Xpert Pro diffractometer using Cu Kα radiations. The structural Rietveld refinements were performed using FULLPROF program incorporated in the WinPLOTR Package. The electrical resistivity and thermopower were measured simultaneously in the temperature range of 350–1000 K using a ULVAC-ZEM3 device under partial Helium pressure. The heat capacity and thermal diffusivity were analyzed using Netzsch DSC 404C and LFA-457 models respectively. The thermal conductivity (κ) was calculated using the product of the geometrical density, the thermal diffusivity and the heat capacity. The lattice thermal conductivity was determined from the Wiedmann–Franz law by subtracting the electronic contribution to the thermal conductivity from the total thermal conductivity ($\kappa_L = \kappa_{total} - \kappa_{elec}$). All the property measurements were performed on the same puck. Scanning electron microscopy and XRD analysis revealed a weak preferential crystallographic orientation of the obtained pellets with the stacking direction (c axis) along the applied pressure direction. Accordingly, the measurements of S, ρ and κ were all performed along the average (ab) planes.

3. Results and discussion

$TiSe_2$ and TiS_2 are known to exhibit the same trigonal crystal symmetry related to the layered CdI_2 structure type, a ubiquitous prototype for AX_2 stoichiometries. The CdI_2 layer is composed of edge-shared octahedra of AX_6 (A: transition metal and X: chalcogen or halogen) that form infinite layers perpendicular to the c axis (Fig. 1). All the structures of the series TiS_xSe_{2-x} ($x = 1$, 1.25, 1.5 and 2) can be well refined in the aristotype space group P-3m1, which implies a statistic distribution of the sulfur and selenium atoms over the same crystallographic site (Ti 1a: 0, 0, 0 and S/Se 2d: 1/3, 2/3, Z). Furthermore, the existence of this solid solution is confirmed by the linear evolution of cell parameters (Fig. 2) that

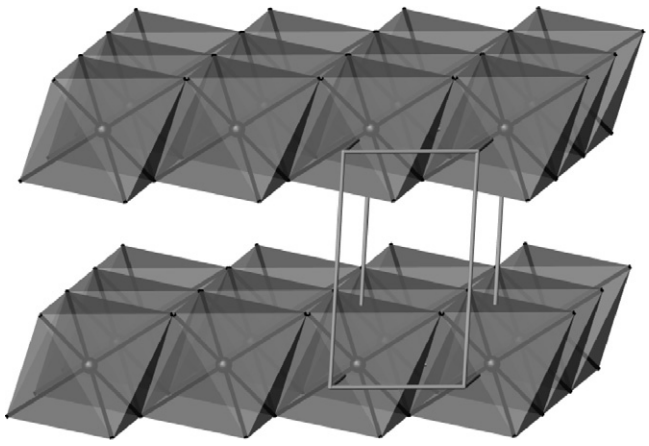

Fig. 1. Representation of the layered CdI_2 type structure of the titled compounds showing the layers made of edge-shared octahedra.

follow Vegard's law with x varying from 0 to 2. Indeed, between the two end members the variation of the volume of the cell is close to 11% with a variation of about −4% within and between plans for x varying from 0 to 2 (ionic radii: 1.84 Å for S^{2-} and 1.98 Å for Se^{2-}). This evidently implies that the spacing separating the TiX_2 layers is larger in the selenide than in the sulfide.

The series of compounds TiS_xSe_{2-x} is stable in air at room temperature and the synthesis of large polycrystalline batches of the title compounds is rather straightforward although it has been reported that single crystals grown *via* iodine vapor transport exhibit very different low temperature electrical resistivity depending on the temperature used for their preparation [26]. However, in the same report, it is also stated that below a temperature of synthesis of 700 °C, the deviation from the 1:2 stoichiometry falls within the measurement uncertainty and also that the use of iodine as transport agent is favorable to the presence of up to 0.3 at.% of iodine in the samples [26]. Thus, using a temperature of 650 °C and no iodine (useless for preparing polycrystalline sample), the substitution of selenium by sulfur is easy to realize and indeed a full solid solution exist between TiS_2 and $TiSe_2$. Scanning electron microscopy and electron dispersive spectroscopy were performed on every sample and confirmed the absence of impurity phase and also the relative ratio of the elements in all the members of the solid solution.

Electronically, TiS_xSe_{2-x} can be simply viewed as made of Ti^{4+} cations and of two divalent counter-ions, xS^{2-} and $(2-x)Se^{2-}$. However, the difference of electronegativity between S and Se leads us to intuitively envisage differences in term of physical and

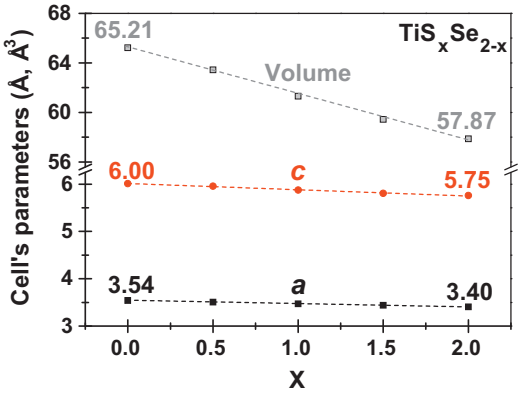

Fig. 2. Evolution of the cell parameters as a function of x in TiS_xSe_{2-x} determined by structural Rietveld refinement.

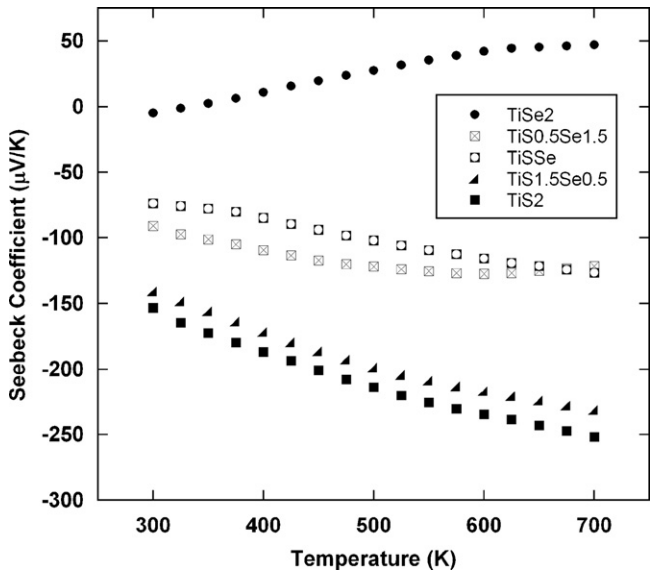

Fig. 3. Evolution of the Seebeck coefficient as a function of temperature for TiS_xSe_{2-x} with $x = 0$, 0.5, 1.0, 1.5 and 2.

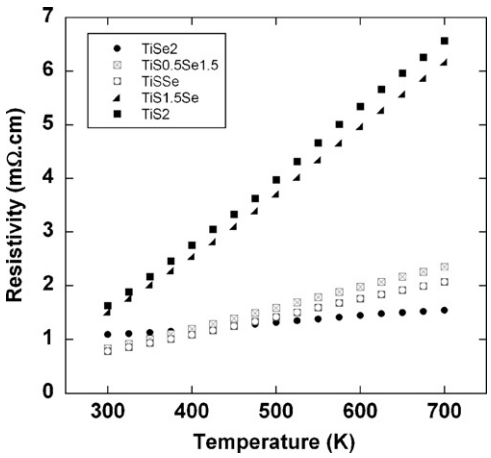

Fig. 4. Evolution of the electrical resistivity as a function of temperature for TiS_xSe_{2-x} with $x = 0$, 0.5, 1.0, 1.5 and 2.

chemical properties. Indeed, the more electronegative sulfur renders the structure of TiS_2 more ionic than that of $TiSe_2$, so that a larger electrical resistivity is expected for the sulfide, together with a larger Seebeck coefficient. Behind that rather "chemical" view, lays the question of the respective band gaps of TiS_2 and $TiSe_2$, and according to the numerous reports on that topic, the question is still not firmly resolved, although band gaps have been attributed for both compounds [25,27–31].

Indeed, these underlined differences are reflected on the transport properties. In Table 1 are reported the transport properties at room temperature and at 700 K of all TiS_xSe_{2-x} with $x = 0$, 0.5, 1, 1.5, and 2. The positive sign of the Seebeck coefficient of $TiSe_2$ is reminiscent of a p-type material while TiS_2 is clearly n-type (Fig. 3). Moreover the amplitude and the slope of the Seebeck coefficient data also indicates a pronounced degree of metallicity of the selenide as reported before, while the large thermopower of the sulfide is rather providing evidences for its semiconducting behavior (Fig. 3). It is worth noticing that the room temperature thermopower reported in this paper (−153 μV/K), compares very well with the value reported in a previous study [18]. Throughout the solid solution, the values of the Seebeck coefficient are expected to fall in between the values measured for the two end-members. It is indeed the case as the n-type behavior is reinforced by the substitution of selenium by sulfur. This can very simply be attributed to the fact that sulfur is a much "better" anion than selenium, so that it provides more electrons to the structure, hence behaving like an n-type dopant. In Fig. 3, it is also noticeable that the compound $TiS_{0.5}Se_{1.5}$ behaves somewhat differently than the sulfur-richer member of the solid solution as its Seebeck coefficient seems to reach a pick value around 570 K before decreasing, whereas all the other compounds have strictly monotonically increasing thermopower with temperature (in absolute value).

The electrical resistivity of all the compounds increases monotonically with increasing temperature, feature typical of (semi)-metal or heavily doped semiconductors. Indeed while TiS_2 shows a resistivity ranging from 1.63 mΩ cm to 6.56 mΩ cm from room temperature to 700 K, the more metallic $TiSe_2$ has a lower resistivity that furthermore has little variation with temperature as shown in Fig. 4.

The thermal conductivity (Fig. 5) of TiS_2 and $TiSe_2$ is varying as a function of T^{-x} and decreases from 3.4 and 5.5 W/mK at room temperature to 2.1 and 4.8 W/mK at 700 K for the sulfide and the selenide, respectively. Except for $TiS_{0.5}Se_{1.5}$, the other members of the solid solution have lower thermal conductivity than TiS_2, due to the disorder generated by the mix occupancy of S and Se. Fig. 6 represents the lattice thermal conductivity at 300 K of TiS_xSe_{2-x} as a function of x. As expected from the theory, the minimum thermal conductivity is obtained for TiSSe corresponding to an equi-molar ratio of anions. The lattice thermal conductivity of each compound at 700 K is also shown in Fig. 6, it is lower than at room temperature and with a value of 1.1 W/mK, TiS_1Se_1 has the lowest thermal conductivity of all. Here again, the somewhat "different" transport properties behavior of $TiS_{0.5}Se_{1.5}$ should be stressed out. In order to validate these data and erase any doubt concerning the actual stoichiometry and purity of this particular sample, the same composition has been synthesized and analyzed several times and undoubtedly the same composition and measured data were obtained each time. This rather peculiar variation of properties with temperature may be due to the fact that this compound might be situated just at the border of the two different regimes observed for TiS_2 and $TiSe_2$ that show an n-type and a p-type character, respectively. Band structure calculations might be useful to clarify this behavior. This "anomalous composition" is also very different from

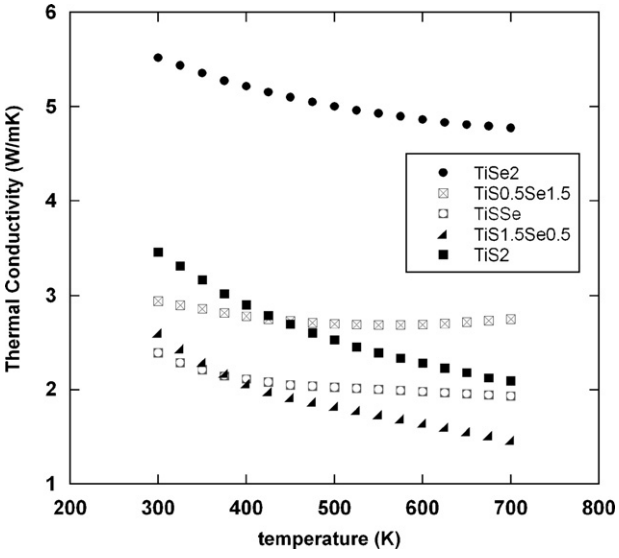

Fig. 5. Evolution of the total thermal conductivity as a function of temperature for TiS_xSe_{2-x} with $x = 0$, 0.5, 1.0, 1.5 and 2, calculated by multiplying the measured thermal diffusivity by the density and by the Dulong–Petit specific heat.

Table 1
Seebeck coefficient, electrical resistivity, thermal conductivity, power factor and thermoelectric figure of merit at 300 K and 700 K for the compounds TiS_xSe_{2-x} with $x = 0$, 0.5, 1, 1.5 and 2.

	TiS_2		$TiS_{1.5}Se_{0.5}$		TiSSe		$TiS_{0.5}Se_{1.5}$		$TiSe_2$	
Temperature (K)	300	700	300	700	300	700	300	700	300	700
Resistivity (mΩ cm)	1.63	6.56	1.52	6.17	0.78	2.07	0.83	2.35	1.09	1.54
Seebeck (μV/K)	−153	−252	−141	−231	−73	−126	−91	−121	−5	47
Power factor (mW/mK^2)	1.64	0.85	1.30	0.86	0.69	0.77	0.99	0.62	0.002	0.14
Thermal conductivity (W/mK)	3.45	2.09	2.60	1.46	2.39	1.93	2.94	2.75	5.52	4.77
ZT	0.12	0.33	0.15	0.41	0.09	0.28	0.10	0.16	10^{-4}	0.02

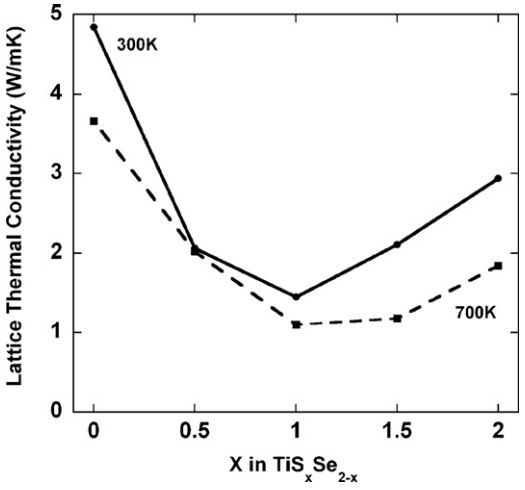

Fig. 6. Evolution of the lattice thermal conductivity as a function of x in TiS_xSe_{2-x} at 300 K and at 700 K.

the other compositions in term of figure of merit, as it is the only one that passes through a maximum value at about 600 K while the other compounds have monotonically increasing zT over the all range of temperature (Fig. 7). $TiSe_2$ has a very low zT owing to its semi-metallic character while a maximum figure of merit of about 0.4 is obtained for $TiS_{1.5}Se_{0.5}$ mostly because of its low thermal conductivity compared to the other compounds while they all have about the same power factor at 700 K (except for $TiSe_2$) as indicated in Table 1.

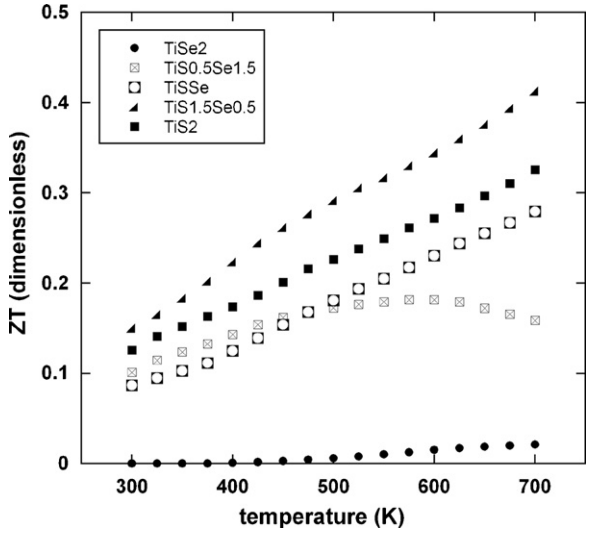

Fig. 7. Evolution of the thermoelectric figure of merit zT as a function of temperature for TiS_xSe_{2-x} with $x = 0$, 0.5, 1.0, 1.5 and 2.

4. Conclusion

Within the large family of AX_2 compounds, two main structure-types coexist depending on the nature of the component, CdI_2 with hexagonal coordination and MoS_2 with prismatic coordination. Moreover, some compositions do not exist without the presence of an intercalated species filling the interlayer spacing, for example, $CrSe_2$ is not stable while $AgCrSe_2$ consists of CdI_2 layers of $CrSe_2$ with silver atoms between the layers. The title compound indeed exists without intercalated species but can also accommodate numerous chemical entities. Such a variety of possible combination is indeed an attractive playground for seeking adequate transport properties and eventually tuning them into efficient thermoelectric properties. Our present report shows that the "empty" structures along the solid solution TiS_xS_{2-x} (no species within the interlayer spacing) have reasonable thermoelectric properties with a maximum zT of about 0.4 at 700 K. Moreover, the fact that the power factor is higher at the lower temperature (see supplementary information) implies that more effort should be dedicated to lower the thermal conductivity of these layered structures around the ambient. If this can be achieved, transition metal layered lighter chalcogenides might represent a replacement solution to the long known and used bismuth telluride that seems to suffer from the somewhat erratic price of the tellurium, and also from its relatively high density.

Acknowledgment

The authors would like to thank the IdsFundmat project for the financial support of R.N. through an Erasmus mundus fellowship.

Appendix A. Supplementary data

Supplementary data associated with this article can be found, in the online version, at doi:10.1016/j.jallcom.2012.01.067.

References

[1] L.E. Bell, Science 321 (2008) 1457–1461.
[2] S. Brown, F. Gascoin, G.J. Snyder, S.M. Kauzlarich, Chem. Mater. 18 (2006) 1873.
[3] E.S. Toberer, C.A. Cox, S. Brown, T. Ikeda, A. May, S.M. Kauzlarich, G.J. Snyder, Adv. Funct. Mater. 18 (2008) 2795–2800.
[4] S. Brown, E. Toberer, T. Ikeda, C. Cox, F. Gascoin, S.M. Kauzlarich, G.J. Snyder, Chem. Mater. 20 (2008) 3412.
[5] E. Toberer, S. Brown, T. Ikeda, S.M. Kauzlarich, G.J. Snyder, Appl. Phys. Lett. 93 (2008) 062110.
[6] J. Rauscher, C. Cox, T. Yi, C.M. Beavers, P. Klavins, E. Toberer, G.J. Snyder, S.M. Kauzlarich, Dalton Trans. 39 (2010) 1055.
[7] F. Gascoin, S. Ottensmann, D. Stark, S.M. Haile, G.J. Snyder, Adv. Funct. Mater. 15 (2005) 1860.
[8] C.L. Condron, F. Gascoin, G.J. Snyder, S.M. Kauzlarich, J. Solid State Chem. 179 (2006) 2252.
[9] Q.G. Cao, H. Zhang, M. Tang, X. Chen, X. Yang, Y. Grin, J.T. Zhao, J. Appl. Phys. 107 (2010) 053714.
[10] E. Toberer, A. May, B. Melot, E. Flage-Larsen, G.J. Snyder, Dalton Trans. 39 (2010) 1046–1054.
[11] H. Zhang, M. Baitinger, M. Tang, Z. Man, H. Chen, X. Yang, Y. Liu, L. Chen, Y. Grin, J.T. Zhao, Dalton Trans. 39 (2010) 1101–1104.
[12] H. Zhang, J.T. Zhao, Y. Grin, X. Wang, M. Tang, Z. Man, H. Chen, X. Yang, J. Chem. Phys. 129 (2008) 164713.

[13] T. Zhou, B. Lenoir, M. Colin, A. Dauscher, R.A. Al Orabi, P. Gougeon, M. Potel, E. Guilmeau, Appl. Phys. Lett. 98 (2011) 162106.
[14] C. Wan, Y. Wang, N. Wang, W. Norimatsu, M. Kusunoki, K. Koumoto, J. Electron. Mater. 40 (2011) 1271–1280.
[15] E. Guilmeau, Y. Bréard, A. Maignan, Appl. Phys. Lett. 99 (2011) 052107.
[16] L.D. Zhao, D. Berardan, Y.L. Pei, C. Byl, L. Pinsard-Gaudart, N. Dragoe, Appl. Phys. Lett. 97 (2010) 092118.
[17] F. Gascoin, A. Maignan, Chem. Mater. 23 (2011) 2510–2513.
[18] W. Xie, X. Tang, Y. Yan, Q. Zhang, T.M. Tritt, Appl. Phys. Lett. 94 (2009) 102111.
[19] Y. Lan, A.J. Minnich, G. Chen, Z. Ren, Adv. Funct. Mater. 20 (2010) 357–376.
[20] E. Savary, F. Gascoin, S. Marinel, Dalton Trans. 39 (2010) 11074–11080.
[21] T. Ikeda, S.M. Haile, H. Azizgolshani, F. Gascoin, V.A. Ravi, G.J. Snyder, J. Chem. Mater. 19 (2007) 763.
[22] J. Androulakis, C.H. Lin, H.J. Kong, C. Uher, C. Wu, T. Hogan, B.A. Cook, T. Caillat, K.M. Paraskevopoulos, M.G. Kanatzidis, J. Am. Chem. Soc. 129 (2007) 9780–9788.
[23] M. Wang, Y. Zhang, M. Muhammed, Nanostruct. Mater. 12 (1999) 237–240.
[24] J.P. Heremans, V. Jovovic, E.S. Toberer, A. Saramat, K. Kurosaki, A. Charoenphakdee, S. Yamanaka, G.J. Snyder, Science 321 (2008) 554–557.
[25] Y. Pei, X. Shi, A. LaLonde, H. Wang, L. Chen, G.L. Snyder, Nature 473 (2011) 66–69.
[26] F.J. Di Salvo, D.E. Moncton, J.V. Waszczak, Phys. Rev. B 14 (1976) 4321.
[27] H.W. Myron, A.J. Freeman, Phys. Rev. B 11 (1974) 481.
[28] J.A. Wilson, Solid State Commun. 22 (1977) 551.
[29] A.H. Reshak, S. Auluck, Phys. Rev. B 68 (2003) 245113.
[30] M. Zabernik, K. Chashka, L. Patlgan, A. Maniv, C. Baines, P. King, A. Kanigel, Phys. Rev. B 81 (2010) 220505.
[31] B. Liu, J. Yang, Y. Han, T. Hu, W. Ren, C. Liu, Y. Ma, C. Gao, J. Appl. Phys. 109 (2011) 053717.